

38. GEOCHEMICAL HISTORY OF POST-JURASSIC SEDIMENTATION IN THE CENTRAL NORTHWESTERN PACIFIC, SOUTHERN HESS RISE, DEEP SEA DRILLING PROJECT SITE 466¹

I. M. Varentsov, Geological Institute of the U.S.S.R. Academy of Sciences, Moscow, U.S.S.R.

ABSTRACT

Deep Sea Drilling Project Hole 466 was drilled in a small structural depression on southern Hess Rise, about 50 km northeast of Site 465. Identification of the stages in geochemical history of sedimentation in the region of Site 466 is based on interpretation of data on distribution of main components and heavy metals and forms of their occurrences (results of factor analysis and mineralogy), and rates of component accumulation, within the general context of information on these deposits.

Late Albian (early-oceanic). The remarkable geochemical feature of this stage is that the major part of the main components and heavy metals accumulated as basaltic volcanoclastics and clay products of their alteration. The volcanoclastic material is closely bound to sapropelic organic matter. Shallow-water carbonate turbidite sediments play a geochemically insignificant part. The sediments accumulated in a shallow-water basin with stagnant bottom waters. There is hiatus from Upper Albian to upper Turonian.

Late Cretaceous (Turonian/Coniacian-early Maastrichtian). Within this stage were accumulated nannofossil carbonate oozes similar in their geochemistry to pelagic oceanic sediments. The increased rates of sedimentation during the late Turonian-early Santonian can be explained by the model suggesting that the region at that time was situated within the equatorial zone of high biological productivity, during northward movement of the Pacific Plate (Lancelot and Larson, 1975; Lancelot, 1978; van Andel, 1974).

Tertiary-Quaternary. There is a hiatus from late Maastrichtian to early Eocene. In the middle to late Eocene were accumulated pelagic nannofossil carbonate sediments with high contents of materials which remained after dissolution: Mn hydroxides, Al₂O₃, and P compounds. There is a hiatus from early Oligocene to late Miocene. Pelagic nannofossil oozes accumulated during the early Pliocene to Pleistocene have relatively high concentrations of SiO₂, Al₂O₃, Fe, Mn, and associated heavy metals, increasing towards the Pleistocene because of intensification of island volcanism.

The geochemical stages of post-Jurassic sedimentation in the region concerned, as for some other areas of the northwestern Pacific, reflect the evolution of the basin, from relatively shallow-water environments with essential influence of volcanism during early stages to pelagic conditions of the open ocean.

INTRODUCTION

Hole 466 was drilled in a small structural depression of Southern Hess Rise (northeastern Mellish Bank), about 50 km northeast of Site 465 (see Site 466 report, this volume). Such a position of the section permits us to compare both regional and local factors which caused the history of sedimentation at its different stages, and among other things gives insight into the nature of some hiatuses, facies changes, rates of sedimentation, persistence of sediment composition, etc.

This paper succeeds a number of works on the geochemical history of post-Jurassic sedimentation in the central northwestern Pacific, drilled during DSDP Leg 62 (see papers by Varentsov et al., this volume, on Sites 463, 464, and 465). As in the previous works, the main objective was to reveal the geochemical history, registered in the chemical and mineral composition of sediments, based on study of the chemistry of main components, heavy metals, trace elements, mineralogy, and lithology.

MATERIALS AND METHODS

The study is based on the data of chemical and mineral composition of sediments recovered from Hole 466, analyzed at the Geological Institute of the U.S.S.R. Academy of Sciences.

Data on mineralogy and lithology of deposits are given in other parts of this volume.

A detailed description of methods was given in the paper on Site 463 (Varentsov et al., this volume). It should be emphasized that the chemical analyses of sediments were made at the Geological Institute of the U.S.S.R. Academy of Sciences, main components by methods of bulk analysis, heavy metals and trace elements by optical emission spectroscopy, by comparison with international reference standards (Zolotarev and Choporov, 1978; Kirkpatrick, 1979).

Methods for recalculation of chemical analysis data into terrigenous-free, carbonate-free, silica-free matter, applied in the works on geochemistry of sediments recovered during Leg 62 were published earlier (Varentsov and Blazhchishin, 1976).

Analytical data were processed by computer (EC-1022) at the Geological Institute of the U.S.S.R. Academy of Sciences (D. A. Kazimirov, P. K. Ryabushkin), according to the program of factor analysis (Davis, 1973; Harman, 1967). Interpretation of analytical data and results of factor analysis was based on the study of mineralogical and lithologic composition of sediments, as slides under the microscope, and by means of X-ray diffraction, whereas composition of clay components of the <0.001-mm fraction are given by Rateev et al. (this volume).

PARAGENETIC ASSOCIATIONS OF COMPONENTS

As mentioned in the previous work on the geochemistry of sediments at Site 463 (Varentsov et al., this volume), the paragenetic associations of chemical components are inferred from interpreted factor analysis data, taking into account all data on mineralogy and lithology.

¹ Initial Reports of the Deep Sea Drilling Project, Volume 62.

Data on Chemical Analysis (Tables 1, 2, 3; Fig. 1)

Association IA (+): $\text{SiO}_2(0.21)\text{-MgO}(0.19)\text{-C}_{\text{org}}(0.84)\text{-P}(0.58)\text{-Cr}(0.98)\text{-Ni}(0.99)\text{-V}(0.82)\text{-Cu}(0.99)\text{-Pb}(0.11)\text{-Ge}(0.15)\text{-Mo}(0.97)$. This association is represented by basaltic volcanoclastics and products of their transformation: magnesian smectites closely associated with organic carbon, phosphorus, and heavy metals (Cr, Ni, Cu, Mo, V). The association is strictly localized in the section: late Albian olive-gray limestones, considerably enriched in basalt volcanoclastics and sapropelic organic matter. Lithology of these sediments and composition of clay components are shown on Figure 1.

Assemblage IB (-): $\text{CaO}(-0.33)\text{-Na}_2\text{O}(-0.78)\text{-K}_2\text{O}(-0.17)\text{-CO}_2(-0.27)\text{-Mn}(-0.39)$. This assemblage is represented by nannofossil and foraminifer remains composed of calcium carbonate, closely bound with Na derived from sea water. The presence of manganese permits us to assume that some molecules of MnCO_3 resulted from post-sedimentation transformations of volcanoclastics, a silicate admixture, and manganese hydroxide.

The stratigraphic distribution of the assemblage is restricted to Unit I (early Campanian-Pleistocene), represented by nannofossil oozes (Fig. 1), relatively slightly altered.

Assemblage IIA (+): $\text{SiO}_3(0.89)\text{-Al}_2\text{O}_3(0.84)\text{-MgO}(0.61)\text{-Na}_2\text{O}(0.44)\text{-K}_2\text{O}(0.93)\text{-Fe}(0.93)\text{-V}(0.39)\text{-Pb}(0.54)\text{-Ga}(0.30)\text{-Ge}(0.57)$. This assemblage is represented by clay components: illite, chlorite, with an admixture of montmorillonite and kaolinite. It should be emphasized that distribution of the assemblage within the section is almost completely related to the poly-mineralic association of clay components in the lower Pliocene-Pleistocene (Fig. 1).

Assemblage IIB (-): $\text{CaO}(-0.89)\text{-CO}_2(-0.89)\text{-Co}(0.42)$. This assemblage is represented by calcium carbonate, with a relatively small admixture of Co, possibly in the form of CoCO_3 , as an epigenetic product of alteration of volcanoclastic materials.

It is noteworthy that the assemblage relates to the lower part of Unit I, within the same intervals of the sec-

tion (lower Campanian-lower Pliocene) where we observe distinct recrystallization of nannofossil oozes (Fig. 1). The amount of recrystallized calcite in the Sub-unit IB (84.0-245.5 m) is up to 15% (see Site 466 report, this volume); this is reflected in the distribution of density values (cf. site report). Whereas the sediments of Sub-unit IA (0-60 m), which is almost free of this group of components, the average density is $1.48 \pm 0.04 \text{ g/cm}^3$, in Sub-unit IB (60-250 m) a higher average density is found ($1.59 \pm 0.03 \text{ g/cm}^3$). The recrystallization of biogenic carbonate remains is irregular: intervals with factor groupings corresponding to weakly altered nannofossil oozes, IB (-), and products of their recrystallization, IIB (-), overlap the boundaries of Sub-unit IB (Fig. 1).

Assemblage IIIA (+): $\text{Al}_2\text{O}_3(0.36)\text{-Mn}(0.83)\text{-P}(0.69)$. The mineral nature of this group is not clear. The assemblage can be considered as represented by scattered manganese hydroxides remaining after dissolution of fine basaltic volcanoclastics, associated with phosphorous and alumina. This conclusion is confirmed both by the relatively higher concentrations of manganese and other components (Table 1) in the intervals with the prominent values of the assemblage (Samples 7-6, 65-67 cm and 8-3, 18-20 cm), and also by the relatively intense brownish color of these sediments (Site 466 report, this volume).

Localization of this group is noteworthy: relatively high values of factor scores are observed near the Pliocene/late Eocene hiatus, which favors the assumption of a residual nature of the components concerned.

Assemblage IIIB (-): $\text{MgO}(-0.42)\text{-Pb}(-0.36)\text{-Mo}(-0.34)$. This assemblage is represented by magnesian montmorillonite and bound heavy metals, developed after hyalopilitic-silty basaltic volcanoclastics. The samples with relatively high values of factor scores (13-3, 123-125 cm; 15-4, 20-22 cm) reveal rather distinctly the volcanogenic nature of the clay components. It is noteworthy that the samples are localized at the mid-Eocene/early Maastrichtian hiatus. Within the stratigraphic interval concerned are observed scattered fragments and pebbles of alkaline basalts eroded from the

Table 1. Chemical composition of Mesozoic and Cenozoic sediments, central northwestern Pacific, southern Hess Rise, DSDP Site 466.

| Sample (interval in cm) | Components | | | | | | | | | | | | | | (wt. % $\times 10^{-4}$) | | | | | | | | |
|----------------------------|------------------|--------------------------------|--------------------------------|-------|------|------|-------------------|------------------|-----------------|------|-------------------------------|-------------------|-------------------|------------------|---------------------------|-----|-----|-----|-----|-----|----|----|------|
| | (wt. %, air-dry) | | | | | | | | | | | | | | | | | | | | | | |
| | SiO ₂ | Al ₂ O ₃ | Fe ₂ O ₃ | CaO | MgO | MnO | Na ₂ O | K ₂ O | CO ₂ | C | P ₂ O ₅ | Fe _{tot} | Mn _{tot} | P _{tot} | Cr | Ni | V | Cu | Co | Pb | Ga | Ge | Mo |
| 466-1-2, 90-92 | 19.48 | 5.26 | 1.74 | 36.06 | 1.23 | 0.04 | 2.28 | 1.34 | 27.55 | — | 0.09 | 1.22 | 0.03 | 0.04 | 10 | <10 | 30 | <20 | <10 | 11 | <5 | <1 | <1.5 |
| 2-4, 64-66 | 9.58 | 2.78 | 0.92 | 45.13 | 0.70 | 0.04 | 1.77 | 0.78 | 35.25 | — | 0.04 | 0.64 | 0.03 | 0.03 | <10 | <10 | 16 | <20 | <10 | <10 | <5 | <1 | <1.5 |
| 3-4, 48-50 | 5.79 | 1.55 | 0.65 | 49.23 | 0.35 | 0.02 | 1.22 | 0.51 | 38.15 | — | 0.05 | 0.45 | 0.02 | 0.02 | <10 | <10 | <15 | <20 | <10 | <10 | <5 | <1 | <1.5 |
| 4-1, 21-23 | 8.49 | 2.56 | 0.65 | 45.75 | 0.70 | 0.03 | 1.77 | 0.74 | 35.40 | 4.71 | 0.04 | 0.45 | 0.02 | 0.02 | <10 | <10 | <15 | <20 | <10 | <10 | <5 | <1 | <1.5 |
| 5-2, 20-22 | 2.86 | 0.86 | 0.22 | 51.91 | 0.18 | 0.04 | 1.44 | 0.36 | 40.30 | — | 0.06 | 0.15 | 0.03 | 0.03 | <10 | <10 | <15 | <20 | <10 | <10 | <5 | <1 | <1.5 |
| 6-6, 40-42 | 11.42 | 3.23 | 1.48 | 42.86 | 0.97 | 0.06 | 1.77 | 1.00 | 33.60 | — | {0.14 0.16} | 1.04 | 0.05 | {0.06 0.07} | <10 | <10 | <15 | <20 | <10 | <10 | <5 | <1 | <1.5 |
| 7-6, 65-67 | 0.60 | 0.26 | 0.26 | 54.01 | — | 0.07 | 1.22 | 0.05 | 42.55 | — | 0.14 | 0.18 | 0.05 | 0.06 | <10 | <10 | <15 | <20 | <10 | <10 | <5 | <1 | <1.5 |
| 8-3, 18-20 | 4.17 | 0.49 | 0.49 | 51.12 | 0.62 | 0.21 | 0.87 | 0.33 | 41.80 | — | 0.41 | 0.34 | 0.16 | 0.18 | <10 | <10 | <15 | <20 | <10 | <10 | <5 | <1 | <1.5 |
| 9-3, 20-22 | 2.22 | 0.64 | 0.43 | 50.85 | 0.50 | 0.01 | 1.16 | 0.37 | 40.90 | — | 0.12 | 0.30 | 0.01 | 0.05 | <10 | <10 | <15 | <20 | <10 | <10 | <5 | <1 | <1.5 |
| 13-3, 123-125 | 1.74 | 0.01 | 0.13 | 54.04 | 0.33 | — | 1.06 | 0.12 | 42.72 | — | 0.02 | 0.09 | — | 0.01 | <10 | <10 | <15 | <20 | <10 | <10 | <5 | <1 | <1.5 |
| 15-4, 20-22 | 0.26 | — | 0.17 | 53.38 | 0.50 | — | 1.16 | 0.16 | 43.30 | — | 0.04 | 0.12 | — | 0.02 | <10 | <10 | <15 | <20 | <10 | <10 | <5 | <1 | <1.5 |
| 16-2, 22-24 | 0.60 | — | 0.20 | 53.01 | 0.33 | 0.01 | 1.16 | 0.16 | 42.15 | — | 0.04 | 0.14 | 0.01 | 0.02 | <10 | <10 | <15 | <20 | <10 | <10 | <5 | <1 | <1.5 |
| 29-2, 0-1 | 5.28 | 1.28 | 0.44 | 42.03 | 0.33 | — | 0.77 | 0.41 | 32.30 | 7.31 | 0.21 | 0.31 | — | 0.09 | 40 | 47 | 210 | 50 | <10 | <10 | <5 | <1 | 8.5 |
| 30-1, 69-70 | 8.19 | 0.69 | 0.50 | 43.59 | 1.33 | — | 0.77 | 0.24 | 34.35 | 3.81 | 0.25 | 0.35 | — | 0.11 | 37 | 34 | 69 | 41 | <10 | <10 | <5 | <1 | 4.5 |
| 34-1, 106-107 | 6.35 | 0.31 | 0.52 | 45.91 | 0.91 | — | 0.61 | 0.24 | 36.60 | 3.21 | 0.15 | 0.36 | — | 0.07 | 28 | 24 | 49 | 38 | <10 | <10 | <5 | <1 | 3.1 |
| 35-1, 59-60 | 6.35 | 0.31 | 0.52 | 45.91 | 0.91 | — | 0.61 | 0.24 | 38.90 | 2.91 | 0.13 | 0.36 | — | 0.07 | 17 | 23 | 50 | 36 | <10 | <10 | <5 | <1 | 3.0 |

Table 2. Results of factor analysis (R-mode) for chemical components of Mesozoic and Cenozoic sediments, central northwestern Pacific, southern Hess Rise, DSDP Site 466.

| No. | Components | Factor Loadings (after rotation) | | |
|----------------------|--------------------------------|-------------------------------------|-------|-------|
| | | I | II | III |
| 1 | SiO ₂ | 0.21 | 0.89 | |
| 2 | Al ₂ O ₃ | 0.05 | 0.84 | 0.36 |
| 3 | CaO | -0.33 | -0.89 | |
| 4 | MgO | 0.19 | 0.61 | -0.42 |
| 5 | Na ₂ O | -0.78 | 0.44 | |
| 6 | K ₂ O | -0.17 | 0.93 | |
| 7 | CO ₂ | -0.27 | -0.89 | |
| 8 | C _{org} | 0.84 | 0.15 | |
| 9 | Fe | 0.01 | 0.93 | |
| 10 | Mn | -0.39 | 0.17 | 0.83 |
| 11 | P | 0.58 | | 0.69 |
| 12 | Cr | 0.98 | 0.08 | |
| 13 | Ni | 0.99 | 0.08 | |
| 14 | V | 0.82 | 0.39 | |
| 15 | Cu | 0.99 | 0.08 | |
| 16 | Co | -0.03 | -0.42 | |
| 17 | Pb | 0.11 | 0.54 | -0.36 |
| 18 | Ga | | 0.30 | |
| 19 | Ge | 0.15 | 0.57 | -0.34 |
| 20 | Mo | 0.97 | 0.09 | |
| Dispersion input (%) | | 39.58 | 24.46 | 8.84 |
| Dispersion total (%) | | 39.58 | 66.04 | 78.88 |

Table 3. Stratigraphic distribution of factor scores (R-mode) for chemical components (recalculated) in the section of Mesozoic and Cenozoic sediments, central northwestern Pacific, southern Hess Rise, DSDP Site 466.

| No. | Sample (interval in cm) | Stratigraphy | Factor Scores (after rotation) | | |
|-----|----------------------------|--------------|-----------------------------------|-------|-------|
| | | | I | II | III |
| 1 | 1-2, 90-92 | Pleistocene | -0.61 | 2.16 | -0.25 |
| 2 | 2-4, 64-66 | Pleistocene | -0.86 | 1.06 | -0.03 |
| 3 | 3-4, 48-50 | U. Pliocene | -0.66 | 0.28 | -0.66 |
| 4 | 4-1, 21-23 | U. Pliocene | -0.51 | 0.66 | -0.52 |
| 5 | 5-2, 20-22 | L. Pliocene | -0.63 | -0.42 | 0.50 |
| 6 | 6-6, 40-42 | L. Pliocene | -0.75 | 1.39 | 0.83 |
| 7 | 7-6, 65-67 | L. Pliocene | -0.33 | -1.59 | 2.05 |
| 8 | 8-3, 18-20 | U. Eocene | -0.28 | -0.25 | 2.23 |
| 9 | 9-3, 20-22 | U. Eocene | -0.52 | 0.02 | -0.25 |
| 10 | 13-3, 123-125 | U. Campanian | -0.57 | -1.06 | -1.65 |
| 11 | 15-4, 20-22 | U. Campanian | -0.49 | -1.23 | -1.38 |
| 12 | 16-2, 22-24 | L. Campanian | -0.49 | -1.44 | -0.28 |
| 13 | 29-2, 0-1 | U. Albion | 2.31 | 0.43 | 0.22 |
| 14 | 30-1, 69-70 | U. Albion | 1.83 | 0.11 | -0.06 |
| 15 | 34-1, 106-107 | U. Albion | 1.39 | -0.05 | -0.32 |
| 16 | 35-1, 59-60 | U. Albion | 1.16 | -0.09 | -0.41 |

blocks uplifted by that time (cf. site report). Such a position of the sediments favored intensive alteration of volcanoclastic materials (Fig. 1).

Data on Recalculated Chemical Analyses (Tables 4-6; Fig. 2)

Assemblage IA (+): MgO(0.35)-Fe(0.51)-Mn(0.72). Extra amounts of these components occur as polyminer-

alic clays, mainly chlorite and montmorillonite, formed after basaltic volcanoclastics.

Distribution of this assemblage is rather similar to that of the above-mentioned group IIA (+) (Fig. 1), represented by polymineralic clay components (late Pliocene-Pleistocene).

Assemblage IB (-): P(-0.72)-Cr(-0.94)-Ni(-0.95)-V(-0.97)-Cu(-0.98)-Co(-0.85)-Pb(-0.85)-Ga(-0.86)-Ge(-0.86)-Mo(-0.90). Extra amounts of phosphorus and the associated heavy metals are represented predominantly by basalt volcanoclastics and products of their alteration.

Relatively high factor loading values of this group were noted for late Albian deposits (Fig. 2), where volcanoclastic constituents and the clay products after them constitute up to 30%.

Assemblage IIA (+): CaO(0.74)-MgO(0.78)-Fe(0.70)-Mn(0.48)-Mo(0.14). Extra amounts of this assemblage are represented mainly by Ca-Mg-Fe montmorillonite, related to Mn and Mo, formed after basaltic volcanoclastics. The mineral composition of the samples with relatively high factor loading values of this group (Table 6; Fig. 2) confirms this conclusion (Samples 3-4, 48-50 cm; 29-2, 0-1 cm).

Assemblage IIB (-): Na₂O(-0.86)-Co(-0.40)-Pb(-0.41)-Ga(-0.34)-Ge(-0.32). This group is negatively correlated with the above-mentioned Assemblage IIA (+). The available data permit us to think that it is predominantly represented by Na-montmorillonite, the result of alteration of basic volcanoclastics. The assemblage has a distinct localization in the section: it is developed predominantly at relatively large hiatuses (late Albian/early Campanian; late Campanian/late Eocene; late Eocene/early Pliocene).

Assemblage IIIA (+): K₂O(0.91)-Mn(0.30). Hydro-mica components occur both as illite and as separate packets in mixed-layer illite-montmorillonite. Stratigraphic distribution of this group in many ways is similar to that of Assemblages IIA (+) and IIB (-) (Fig. 2), represented by Ca-Fe-Mg-montmorillonite and its sodium varieties. The data indirectly indicate a predominance of mixed-layer forms over illite proper, which is not contrary to the results of X-ray structural analysis of the clay fraction.

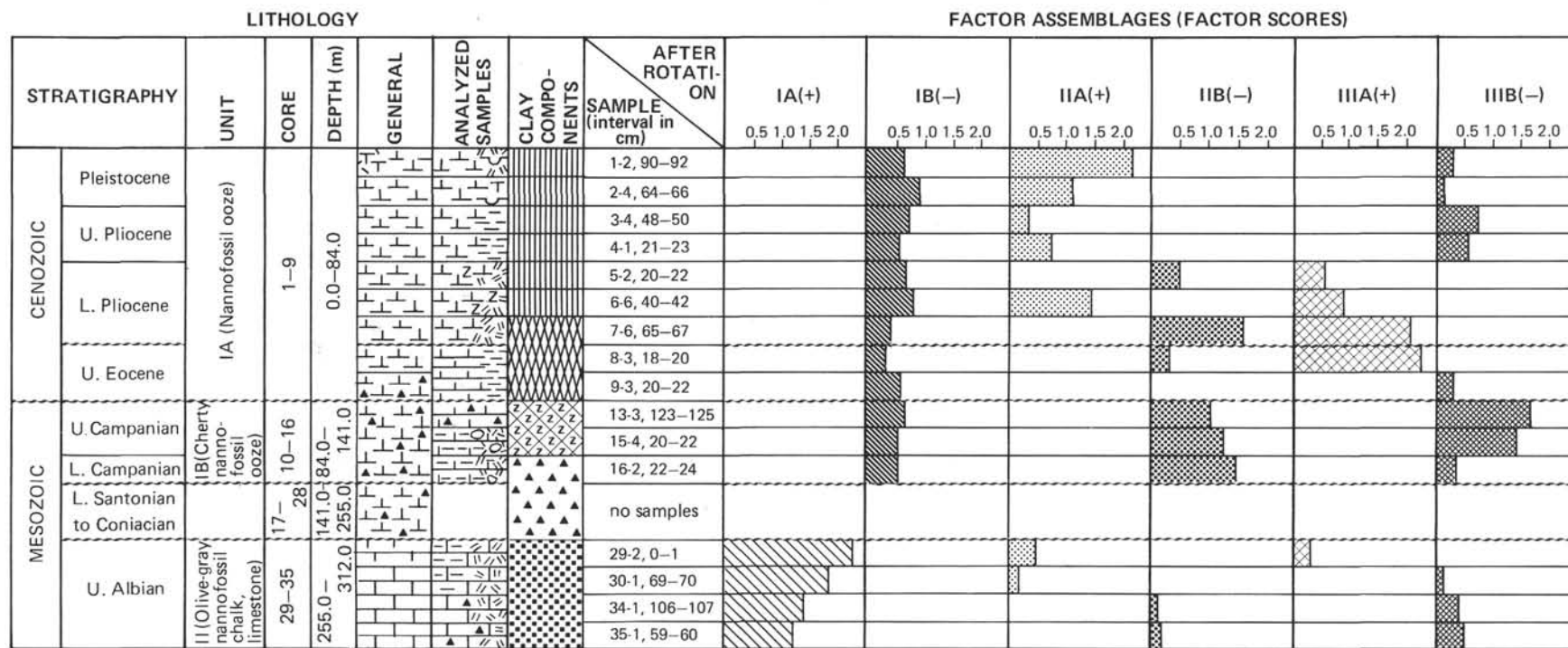
Assemblage IIIB (-): Fe(-0.33). This assemblage represented by excessive amounts of ferric hydroxides, formed during the general process of alteration of basaltic volcanoclastics. The absence of heavy and transition metals in the composition of the group (which are usually associated with hydroxides) indirectly gives evidence of a relatively late, epigenetic formation of this phase.

Of interest is the localization of ferric hydroxides near relatively large hiatuses (Fig. 2).


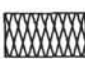



AVERAGE CONTENTS AND ACCUMULATION RATES OF COMPONENTS (Tables 1, 4, 7; Fig. 3-5)

Distribution of Average Contents

The proximity of Sites 466 and 465 is represented in the similarity of main features of lithologic, mineral,



CLAY COMPONENTS

-  Polyminerall assemblage, with illite, chlorite, and an admixture of montmorillonite and kaolinite.
-  Polyminerall assemblage: illite with an admixture of chlorite and mixed-layer montmorillonite-illite.
-  Mixed-layer montmorillonite-illite with zeolite.
-  Cristobalite and tridimite.
-  Fe-montmorillonite with opal-CT and an admixture of mixed-layer montmorillonite-illite.

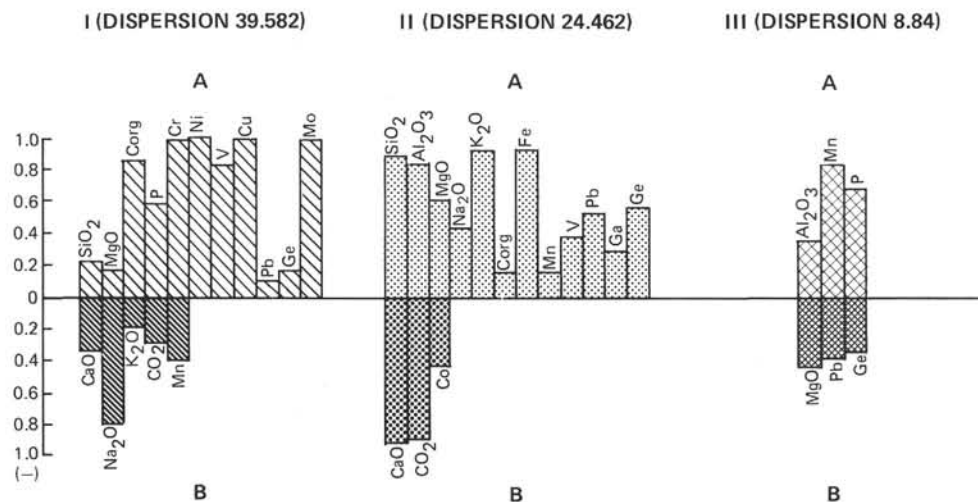


Figure 1. Stratigraphic distribution of factor scores of the main paragenetic assemblages of chemical components (wt. %, air-dry) in the section of Mesozoic and Cenozoic deposits, central northwestern Pacific, southern Hess Rise, DSDP Site 466. Lithologic symbols are those used in DSDP *Initial Reports*.

Table 4. Chemical composition of Mesozoic and Cenozoic sediments, central northwestern Pacific, southern Hess Rise, DSDP Site 466 (wt.%, recalculated to clastic-free, carbonate-free, silica-free).

| Sample (interval in cm) | Components | | | | | | | | | | | | | | | |
|----------------------------|------------|--------|-------------------|------------------|--------|-------|--------|-------|-------|-------|-------|-------|-------|-------|-------|-------|
| | CaO | MgO | Na ₂ O | K ₂ O | Fe | Mn | P | Cr | Ni | V | Cu | Co | Pb | Ga | Ge | Mo |
| 466-1-2, 90-92 | 0.109 | 17.505 | 55.793 | 16.631 | 9.039 | 0.328 | 0.536 | — | — | — | 0.014 | 0.014 | 0.016 | — | 0.001 | 0.003 |
| 2-4, 64-66 | — | 14.786 | 62.526 | 14.976 | 6.462 | 0.798 | 0.342 | — | — | — | 0.046 | 0.027 | 0.027 | 0.004 | 0.003 | 0.005 |
| 3-4, 48-50 | 28.079 | 15.021 | 12.802 | 25.177 | 16.405 | 1.280 | 1.195 | 0.017 | 0.026 | 0.043 | 0.137 | 0.068 | 0.068 | 0.026 | 0.007 | 0.011 |
| 4-1, 21-23 | 8.755 | 15.672 | 56.040 | 15.171 | 3.409 | 0.434 | 0.401 | — | — | 0.003 | 0.047 | 0.027 | 0.027 | 0.007 | 0.003 | 0.009 |
| 5-2, 20-22 | 17.962 | 3.849 | 64.197 | 10.997 | 0.229 | 1.237 | 1.237 | 0.027 | 0.027 | 0.041 | 0.082 | 0.041 | 0.041 | 0.018 | 0.004 | 0.006 |
| 6-6, 40-42 | — | 25.690 | 26.408 | 23.281 | 20.873 | 1.648 | 1.986 | — | — | — | 0.046 | 0.030 | 0.030 | — | 0.003 | 0.005 |
| 7-6, 65-67 | — | — | 87.813 | 1.018 | 6.324 | — | 4.289 | 0.065 | 0.065 | 0.095 | 0.138 | 0.071 | 0.071 | 0.033 | 0.007 | 0.011 |
| 8-3, 18-20 | — | — | 65.469 | 20.227 | — | — | 13.742 | 0.062 | 0.062 | 0.093 | 0.147 | 0.073 | 0.073 | 0.033 | 0.007 | 0.011 |
| 9-3, 20-22 | — | — | 77.110 | 19.158 | — | — | 3.273 | 0.048 | 0.048 | 0.075 | 0.123 | 0.061 | 0.061 | 0.027 | 0.006 | 0.010 |
| 13-3, 123-125 | — | 4.693 | 84.311 | 9.545 | — | — | 0.795 | 0.080 | 0.080 | 0.119 | 0.159 | 0.080 | 0.080 | 0.040 | 0.008 | 0.012 |
| 15-4, 20-22 | — | — | 86.037 | 11.867 | — | — | 1.483 | 0.074 | 0.074 | 0.111 | 0.148 | 0.074 | 0.074 | 0.037 | 0.007 | 0.011 |
| 16-2, 22-24 | — | — | 86.037 | 11.867 | — | — | 1.483 | 0.074 | 0.074 | 0.111 | 0.148 | 0.074 | 0.074 | 0.037 | 0.007 | 0.011 |
| 29-2, 0-1 | 32.031 | 9.448 | 35.972 | 11.721 | 4.749 | — | 4.295 | 0.172 | 0.207 | 1.021 | 0.232 | 0.045 | 0.045 | 0.015 | 0.005 | 0.042 |
| 30-1, 69-70 | — | 54.348 | 32.053 | 6.246 | 1.822 | — | 4.684 | 0.147 | 0.134 | 0.278 | 0.169 | 0.039 | 0.039 | 0.017 | 0.004 | 0.019 |
| 34-1, 106-107 | — | 40.952 | 40.078 | 13.247 | — | — | 4.640 | 0.175 | 0.155 | 0.316 | 0.249 | 0.065 | 0.065 | 0.030 | 0.007 | 0.021 |
| 35-1, 59-60 | — | — | 68.760 | 22.728 | — | — | 6.807 | 0.173 | 0.254 | 0.554 | 0.404 | 0.112 | 0.112 | 0.052 | 0.011 | 0.034 |

Table 5. Results of factor analysis (R-mode) of chemical components (recalculated) in the section of Mesozoic and Cenozoic sediments, central northwestern Pacific, Southern Hess Rise, DSDP Site 466.

| No. | Components | Factor Loadings (after rotation) | | |
|----------------------|-------------------|-------------------------------------|-------|-------|
| | | I | II | III |
| 1 | CaO | 0.07 | 0.74 | |
| 2 | MgO | 0.35 | 0.78 | |
| 3 | Na ₂ O | | -0.86 | |
| 4 | K ₂ O | | | 0.91 |
| 5 | Fe | 0.51 | 0.70 | -0.33 |
| 6 | Mn | 0.72 | 0.48 | 0.30 |
| 7 | P | -0.72 | | |
| 8 | Cr | -0.94 | | |
| 9 | Ni | -0.95 | | |
| 10 | V | -0.97 | | |
| 11 | Cu | -0.98 | | |
| 12 | Co | -0.85 | -0.40 | |
| 13 | Pb | -0.85 | -0.41 | |
| 14 | Ga | -0.86 | -0.34 | |
| 15 | Ge | -0.86 | -0.32 | |
| 16 | Mo | -0.90 | 0.14 | |
| Dispersion input (%) | | 62.30 | 17.79 | 7.91 |
| Dispersion total (%) | | 62.30 | 76.09 | 84.00 |

and chemical composition, and distinctly revealed in the distribution of average contents of components within the section (Fig. 3).

The observed differences are related not so much to the different environments of sedimentation as to the local features of the regional history: block movements, exposures of the sources of local sedimentation material and the eroded areas, redeposition of sediments into the locally restricted basins, etc. These local features of development are most distinctly reflected in lithologic-geochemical characteristics and the magnitude of the hiatuses.

Table 6. Stratigraphic distribution of factor scores (R-mode) for chemical components (recalculated) in the section of Mesozoic and Cenozoic sediments, central northwestern Pacific, southern Hess Rise, DSDP Site 466.

| No. | Sample (interval in cm) | Stratigraphy | Factor Scores (after rotation) | | |
|-----|----------------------------|--------------|-----------------------------------|-------|-------|
| | | | I | II | III |
| 1 | 1-2, 90-92 | Pleistocene | 2.21 | 0.20 | -0.52 |
| 2 | 2-4, 64-66 | Pleistocene | 1.60 | -0.22 | 0.18 |
| 3 | 3-4, 48-50 | U. Pliocene | -0.61 | 1.97 | 1.54 |
| 4 | 4-1, 21-23 | U. Pliocene | 1.13 | 0.61 | 0.23 |
| 5 | 5-2, 20-22 | L. Pliocene | 0.27 | 0.50 | 0.02 |
| 6 | 6-6, 40-42 | L. Pliocene | 1.31 | 0.57 | 0.71 |
| 7 | 7-6, 65-67 | L. Pliocene | -0.26 | -0.77 | -2.80 |
| 8 | 8-3, 18-20 | U. Eocene | -0.48 | -0.95 | 0.68 |
| 9 | 9-3, 20-22 | U. Eocene | -0.12 | -1.13 | 0.57 |
| 10 | 13-3, 123-125 | U. Campanian | -0.38 | -0.75 | 0.11 |
| 11 | 15-4, 20-22 | U. Campanian | -0.26 | -1.23 | 0.26 |
| 12 | 16-2, 22-24 | L. Campanian | -0.26 | -1.23 | 0.26 |
| 13 | 29-2, 0-1 | U. Albian | -1.20 | 1.81 | -0.86 |
| 14 | 30-1, 69-70 | U. Albian | -0.61 | 0.96 | -1.51 |
| 15 | 34-1, 106-107 | U. Albian | -0.97 | 0.30 | 0.15 |
| 16 | 35-1, 59-60 | U. Albian | -1.34 | -0.63 | 1.00 |

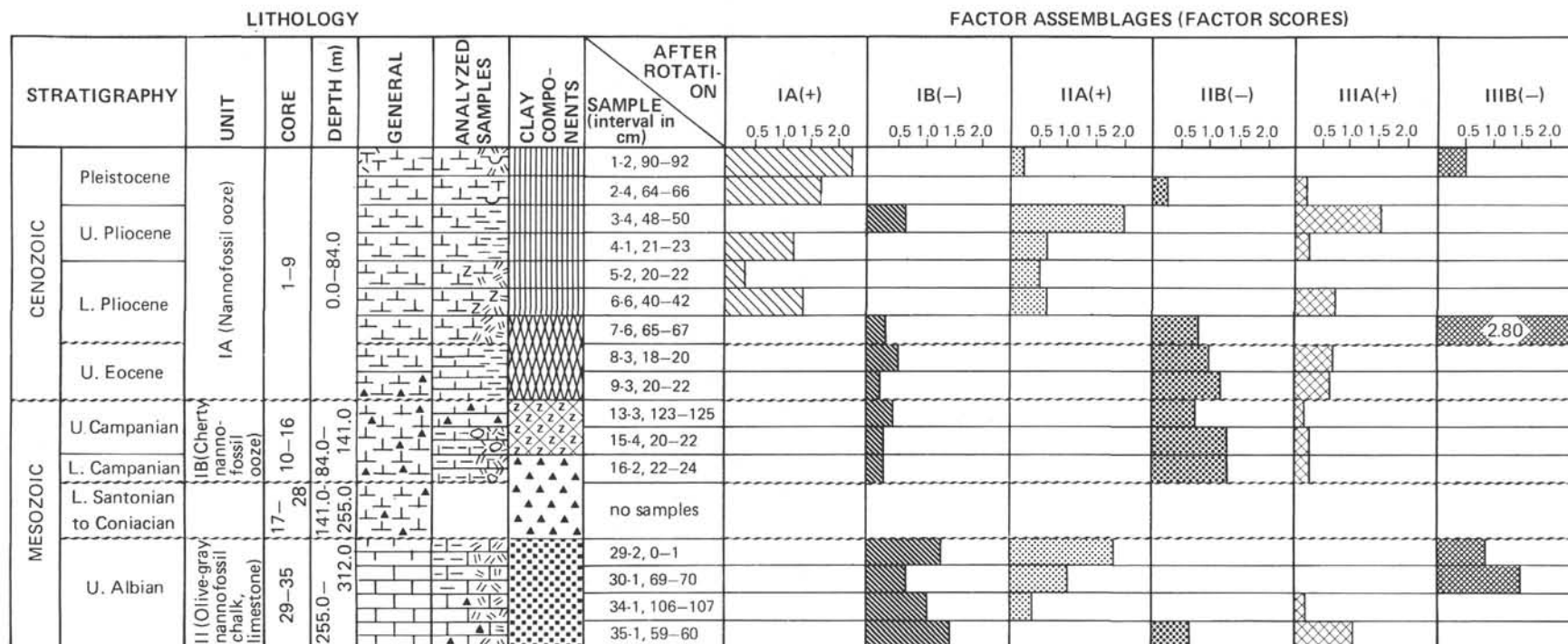
Late Albian (early-oceanic)

The late Albian sediments as in Hole 465 and 465A are characterized by high concentrations of SiO₂, Al₂O₃, Fe, P, C_{org}, and associated heavy metals (Figs. 3 and 4). The low concentrations of Mn and relatively higher contents of normative molecules of FeCO₃ and MgCO₃, related to epigenetic transformation of mafic volcanic material, are noteworthy.




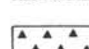

Relatively high concentrations of MgO and K₂O (wt.%, recal.) can be interpreted (Fig. 4) as an indirect indication of the essential part played by initial volcanoclastic material of trachybasalt composition, partially altered to smectite-illite.

Late Cretaceous (late Turonian-Maastrichtian)

The sediments of this stage were rather fragmentarily represented by core samples, and correspondingly by



CLAY COMPONENTS

-  Polyminerall assemblage, with illite, chlorite, and an admixture of montmorillonite and kaolinite.
-  Polyminerall assemblage: illite with an admixture of chlorite and mixed-layer montmorillonite-illite.
-  Mixed-layer montmorillonite-illite with zeolite.
-  Cristobalite and tridimite.
-  Fe-montmorillonite with opal-CT and an admixture of mixed-layer montmorillonite-illite.

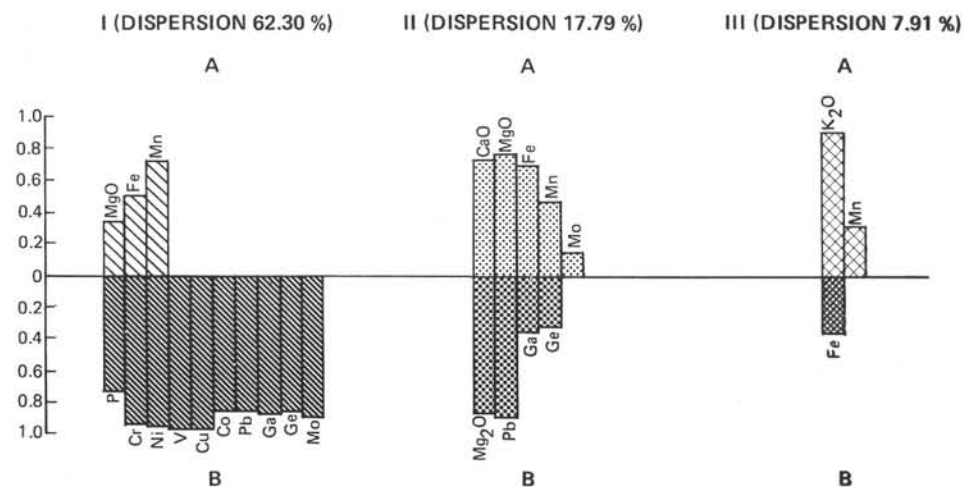


Figure 2. Stratigraphic distribution of factor scores of the main paragenetic assemblages of chemical components (wt. %, recalculated to terrigenous-free, carbonate-free, silica-free) in the section of Mesozoic and Cenozoic deposits, central northwestern Pacific, southern Hess Rise, DSDP Site 466. Symbols as in Figure 1.

chemical analysis. The relatively low concentrations of aluminosilicate components (Campanian sediments are free from Al_2O_3) and the increased amounts of normative MgCO_3 may be read as evidence for considerable epigenetic transformation of carbonate materials (Fig. 3).

Tertiary-Quaternary

These sediments survived two considerable hiatuses (middle Eocene/late Maastrichtian; early Oligocene/late Miocene), and younger deposits show distinct predominance of carbonate nannofossils, with an essential admixture of basaltic volcanoclastics, manifested also in higher concentrations of Al_2O_3 , Fe, Mn, and P. The basal late Eocene sediments reveal (Fig. 3) considerable amounts of normative molecules of MnCO_3 , FeCO_3 , and MgCO_3 as the products of epigenetic alteration of volcanogenic material, while high, excessive amounts of P and K_2O (wt.%, recalculated; Fig. 4) can be interpreted as accumulation of residual materials in the form of biogenic phosphates and illite.

Maximum contents of Al_2O_3 , Fe, Mn, P, and the associated heavy metals in early Pliocene-Pleistocene sediments reflect, as shown earlier (Figs. 1 and 2), the presence of volcanoclastic basaltic components (Figs. 3 and 4).

Rates of Component Accumulation (Table 7; Fig. 5)

Methods of calculation of average linear rates of sedimentation and accumulation of components were discussed in the works on geochemistry of sediments recovered from Holes 463, 464, 465, and 465A during DSDP Leg 62 (Varentsov et al., this volume).

The proximity of Sites 465 and 466 permits estimation of the relationship between regional and local factors in analyzing rates of sedimentation and accumulation of components. However, rather abundant hiatuses resulted in a considerable decrease of deposit thicknesses and corresponding reduction of already minimum rates of sedimentation, which interferes with adequate genetic interpretation of the data. Three stages have been outlined.

Late Albian (early-oceanic)

The early Albian deposits recovered from Holes 465, 465A, and 466 are very close to each other in their facies-genetic nature and geochemical parameters. However, the absence of stratigraphically conformable boundaries between late Albian deposits and underlying and overlying formations (see site reports, this volume) results in a two- to three-fold decrease in the rates of sedimentation and component accumulation compared to these for Holes 465 and 465A. The inconsistency of such data is obvious (Fig. 5).

Late Cretaceous (late Turonian-Maastrichtian)

As mentioned above, Late Cretaceous sediments as a whole show reduction of thickness due to numerous hiatuses. Geochemically, the deposits of Sites 465 and 466 are rather similar.

However, it should be emphasized that the relatively high rates of sedimentation for the late Turonian-early Coniacian and the early Santonian (Fig. 5) can be explained by the model of horizontal northward movement of the Pacific Plate. According to this model (Lancelot and Larson, 1975; Lancelot, 1978; van Andel, 1974), southern Hess Rise could have crossed the equatorial zone of high biological productivity during the Cenomanian-Coniacian, or during an interval close to that. It should be also mentioned that there are two intervals in the record of Holes 465 and 465A which revealed considerably lower three- to four-fold rates of sedimentation compared to Hole 466. However, some intervals, particularly the early Santonian, could have been affected by local redeposition of sediments due to local block displacements, leading to a corresponding increase in rates of sedimentation which took place at that time. Evidence for such local block movements is presented in the site report (this volume).

Tertiary-Quaternary

This stage is represented by middle and late Eocene relict sediments, which survived a considerable hiatus (early Oligocene/late Miocene), and by Pliocene-Pleistocene sediments. The latter show relatively increased (for pelagic sediments) rates of sedimentation (Table 7; Fig. 5) and accumulation of Al_2O_3 , Fe, and Mn. Correlation of rates of sedimentation and accumulation in the late Pliocene-Pleistocene for Sites 465 and 466 shows that on northeastern Mellish Bank sediments were accumulated two- to ten-fold more intensively, while local manifestation of basaltic volcanism resulted in considerable (ten- to twenty-fold) increase of accumulation rates of Al_2O_3 , Fe, and Mn (Fig. 5). As mentioned above, the predominant mode of occurrence of these components in sediments is fine basaltic volcanoclastics. At the same time, the rates of sedimentation and accumulation of the components do not exceed the values, known for carbonate pelagic oozes (Arrhenius, 1963, 1967; Bezrukov and Romankevich, 1970; Bogdanov and Chekhovskikh, 1979; Lisitzin, 1974, 1978; MacArthur and Elderfield, 1977).

GEOCHEMICAL HISTORY OF SEDIMENTATION

Identification of stages reflecting the main events in the geochemical history of post-Jurassic sedimentation in the Hess Rise region was based on analysis of distribution of concentrations of the main components and heavy metals, forms of their occurrences, and rates of accumulation.

Late Albian (early-oceanic)

Within this stage sediments accumulated which are represented (in the studied samples) by thinly laminated, olive-gray limestones, with subordinate amounts of gray limestones, containing abundant (20–30%) basaltic volcanoclastics and sapropelic organic matter (C_{org} to 8–10%, mean 4.31%).

As mentioned above, the lithologic, mineralogical, and facies characteristics of these deposits are similar to

Table 7. Average contents and average rates of accumulation of chemical components for the major geochronological subdivisions of the section of post-Jurassic sediments, central northwestern Pacific, southern Hess Rise, DSDP Site 466.

| Lithologic Unit | Lithology | Core | Sub-bottom Depth (m) | Thickness (m) | Stratigraphy | Core | Sub-bottom Depth (m) | Thickness (m) | Density (g/cm ³) | Water Content (%) | Duration (m.y.) |
|-----------------|--|-------------|----------------------|---------------|---|---------------------|----------------------|---------------|------------------------------|-------------------|-----------------|
| IA | Nannofossil ooze | 1-9 | 0-84.0 | 84.0 | Pleistocene | 0 to 3-1, 20 cm | 0.0-17.7 | 17.7 | 1.48 | 42.9 | 1.8 |
| | | | | | U. Plioc. | 3-1, 20 cm to 4,CC | 17.7-36.5 | 18.8 | 1.48 | 42.9 | 1.0 |
| | | | | | L. Plioc. | 5-1 to 8-1, 90 cm | 36.5-65.9 | 29.4 | 1.48 | 42.9 | 2.0 |
| | | | | | U. Eocene | 8-1, 90 cm to 9,CC | 65.9-84.0 | 18.1 | 1.48 | 42.9 | 3.0 |
| IB | Siliceous nannofossil ooze | 10-27 | 84.0-245.5 | 161.5 | M. Eocene | 10-1 to 10,CC | 84.0-84.2 | 0.2 | 1.48 | 36.7 | 9.0 |
| | | | | | L. Maastr.-U. Campanian | 11-1 to 11,CC | 88.0-93.5 | 5.5 | 1.59 | 36.7 | 2.5 |
| | | | | | U. Campanian | 12-1 to 15,CC | 93.5-131.5 | 38.5 | 1.59 | 36.7 | 4.0 |
| | | | | | L. Campanian | 16-1 to 16-2, 60 cm | 131.5-135.0 | 3.5 | 1.59 | 36.7 | 4.0 |
| | | | | | L. Santon. | 16-2, 60 cm to 2,CC | 135.0-179.0 | 44.0 | 1.59 | 36.7 | 2.0 |
| | | | | | Coniacian/Turonian-L. Santonian/U. Turon. | 21-1 to 27,CC | 179.0-245.5 | 66.5 | 1.59 | 36.7 | } 6.0 |
| Coniac.-Turon. | 28-1 to 28,CC | 245.5-255.0 | 9.5 | 2.30 | 10.3 | | | | | | |
| II | Olive-gray nannofossil chalk and limestone | 28-35 | 245.5-312.0 | 66.5 | U. Albian | 29-1 to 35,CC | 255.0-312.0 | 57.0 | 2.30 | 10.3 | = 4.0 |

those observed in the equivalent sediments recovered from Holes 465 and 465A (Varentsov, this volume). In the section concerned, at least early Cenomanian and partially late Albian sediments, found at adjacent Site 465 of Hess Rise, were eroded.

The most essential feature of sedimentation during this stage resides in the fact that the major part of the main components and heavy metals was accumulated in a form of basaltic volcanoclastics altered to Fe-montmorillonite and mixed-layer illite-montmorillonite. Sapropelic matter is closely bound with the volcanogenic products. Intensive rates of organic matter accumulation in this shallow basin of the depression type, with stagnant bottom waters, were caused by high biological productivity of its planktonic zone. The development of the latter was favored by the contribution of nutrient mineral components of volcanic origin to the basin. Post-sedimentary transformations resulted in formation of geochemical Assemblage IA (+) of main components, heavy metals, and organic matter (Fig. 1; Tables 1-7). Accumulation of carbonate shallow-water sediments of turbidite origin proper played a relatively less-considerable geochemical part.

The rates of sediment accumulation in the sequence concerned could not be adequately assessed; however, correlation with the data on Holes 465 and 465A permits us to conclude that they had high values, typical of a proto-oceanic stage of basin development (Tiercelin and Faure, 1978).

Hiatus (early Cenomanian/middle Turonian)

This hiatus is rather widely distributed over the Hess Rise region; however, its geochronological continuity and erosional activity were caused considerably by local block movements and paleo-hydrodynamic features

(Varentsov, this volume). The hiatus of the region concerned was probably associated with the development of Late Cretaceous analogues of the sub-equatorial currents and their northwestern branches (Luyendyk et al., 1972).

Late Cretaceous (late Turonian/early Maastrichtian)

Accumulation of pelagic nannofossil sediments was broken by a late Santonian hiatus. Geochemical parameters of these sediments are similar to those of pelagic carbonate oozes. Diagenetic-epigenetic recrystallization of the carbonates is of interest in Assemblage IIB (-) (Fig. 1).

Relatively high rates of sediment accumulation during the late Turonian-early Santonian can be interpreted on the basis of the model describing northward movement of the Pacific Plate (Lancelot and Larson, 1975; Lancelot, 1978; van Andel, 1974). According to this model, southern Hess Rise could have been positioned within the zone of high biological productivity during the Cenomanian-Coniacian, or close intervals. On the other hand, alkaline basalt pebbles in late Campanian carbonate sediments can throw light on the role of local contributors of sediments and redeposition of sedimentary materials in the limited graben-like basins.

Tertiary-Quaternary

Hiatus (late Maastrichtian-early Eocene)

This hiatus is of a wide regional nature, reflecting essential changes of the global oceanic paleo-circulation. However, relatively the considerable temporal magnitude of the hiatus and its distinct erosional features compared to the adjacent section of Holes 465 and 465A show (Varentsov, this volume) the significant

Table 7. (Continued).

| Rates of Sedimentation | | Content (wt.%) and Accumulation Rates of Components ($\text{mg}\cdot\text{cm}^{-2}\cdot 10^{-3}\cdot\text{yr}^{-1}$) | | | | | | | | | | | |
|---|--|--|-----------|--------------------------------|-----------|-------------------|-----------|------|-----------|------|-----------|------|-----------|
| ($\text{mm}\cdot 10^{-3}\cdot\text{yr}^{-1}$) | ($\text{mg}\cdot\text{cm}^{-2}\cdot 10^{-3}\cdot\text{yr}^{-1}$) | SiO ₂ | | Al ₂ O ₃ | | CaCO ₃ | | Fe | | Mn | | P | |
| | | (%) | Acc. Rate | (%) | Acc. Rate | (%) | Acc. Rate | (%) | Acc. Rate | (%) | Acc. Rate | (%) | Acc. Rate |
| 9.83 | 1032 | 14.53 | 149.9 | 4.02 | 41.5 | 71.42 | 737.1 | 0.93 | 9.6 | 0.03 | 0.31 | 0.03 | 0.31 |
| 18.8 | 1976 | 7.14 | 141.1 | 2.06 | 40.7 | 83.65 | 1652.9 | 0.45 | 8.9 | 0.01 | 0.2 | 0.02 | 0.39 |
| 14.7 | 1545 | 4.97 | 76.8 | 1.45 | 22.4 | 88.16 | 1362.1 | 0.46 | 7.1 | 0.05 | 0.8 | 0.05 | 0.77 |
| 6.03 | 634 | 3.20 | 20.3 | 0.57 | 3.6 | 90.99 | 576.9 | 0.32 | 2.0 | 0.09 | 0.6 | 0.11 | 0.70 |
| 0.02 | 2.22 | — | — | — | — | — | — | — | — | — | — | — | — |
| 2.20 | 269 | — | — | — | — | — | — | — | — | — | — | — | — |
| 9.5 | 1159 | 1.00 | 11.6 | — | 0 | 95.85 | 1110.9 | 0.10 | 1.2 | — | 0.00 | 0.01 | 0.12 |
| 0.88 | 108 | 0.60 | 0.6 | — | 0 | 94.60 | 102.2 | 0.14 | 0.2 | 0.01 | 0.01 | 0.02 | 0.02 |
| 22.96 | 2681 | — | — | — | — | — | — | — | — | — | — | — | — |
| 12.29 | 2167 | — | — | — | — | — | — | — | — | — | — | — | — |
| 14.25 | 3131 | 6.54 | 204.8 | 0.65 | 20.4 | 78.78 | 2466.6 | 0.34 | 10.6 | — | 0.00 | 0.08 | 2.50 |

part played by a number of local factors (particularly paleo-circulation, bottom geomorphology, block movements, etc.), favoring development of the hiatus.

Middle-Late Eocene

The accumulated sediments are of reduced thickness and are distinctly relict. This is evidenced by higher concentrations of products remaining after dissolution: Mn-hydroxides and components of Al₂O₃ and P in Assemblage IIIA (+) (Fig. 1), related to the erosional boundary of late Eocene sediments. This conclusion is also confirmed by the mixed composition of faunal assemblages, which contain redeposited forms (cf. site report, this volume).

Hiatus (early Oligocene-late Miocene)

This hiatus is of a wide regional nature for the central northwestern Pacific. The temporal magnitude of the hiatus was caused by the relationships of the above-mentioned local factors.

Early Pliocene-Pleistocene

Within this phase were accumulated pelagic, predominantly nannofossil oozes (remains of foraminifers, avg. 4-5%), diatoms (avg. 2-4%), radiolarians (avg. 3-4%), spicules of sponges, and silicoflagellates. Fine (hyalopelite, silty) volcanoclastics of predominantly basaltic, and less frequently acid composition make up 10% in some horizons.

The characteristic features of these sediments are the high concentrations of SiO₂, Al₂O₃, Fe, Mn, and associated heavy metals, increasing from early Pliocene to the Pleistocene (Figs. 3 and 4). The interpretation of factor-analysis data in the context of mineralogy and lithology shows that during this period the main com-

ponents and heavy metals accumulated mainly in the form of volcanoclastics in Assemblages IIA (+) (Fig. 1) and IA (+) (Fig. 2), considerably transformed into polymineralic clay products: illite and chlorite, with an admixture of montmorillonite and kaolinite. Besides the contribution of these components from volcanic sources and authigenic genesis, some could have been supplied as eolian and terrigenous material. However, the predominance of volcanogenic components is obvious. This geochemical feature is reflected in the distribution of accumulation-rate values for SiO₂, Al₂O₃, Fe, and Mn (Fig. 5). Whereas in the phase concerned the highest rates of sedimentation and correspondingly accumulation of CaCO₃ are noted in the late Pliocene, the accumulation of SiO₂, Al₂O₃, Fe, and other components successively increased from the early Pliocene to the Pleistocene, because of activation of island volcanism. Higher rates of accumulation for Mn and P during the early Pliocene were caused by the basal position of these sediments: Mn and P compounds accumulated predominantly as products of dissolution in Assemblage IIIA (+) (Figs. 1 and 5), above a relatively considerable hiatus (early Oligocene/late Miocene).

CONCLUSIONS

Hole 466 was drilled in a small structural depression in southern Hess Rise, about 50 km northeast of Site 465. Such a position of the section permits us to compare the role played by regional and local factors in the formation of sediments, among the other things the features of their chemical composition at different stages of the sedimentation history.

Subdivision of main stages and phases in the geochemical history of Site 466 is based on interpretation of data on distribution of main components, heavy metals,

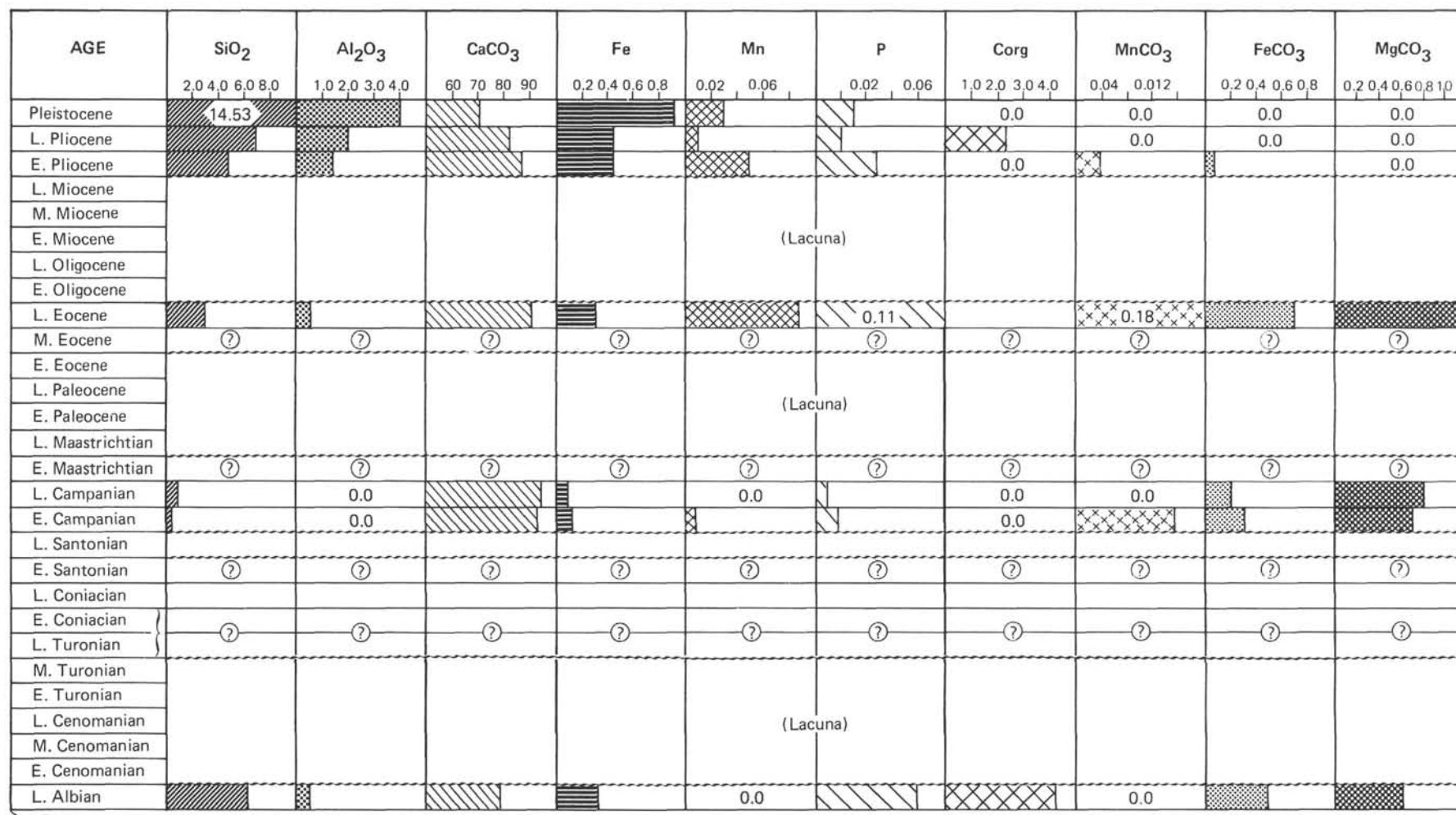


Figure 3. Distribution of average contents (wt. %, air-dry) of SiO₂, Al₂O₃, Fe, Mn, P, and normative molecules of CaCO₃, MnCO₃, FeCO₃, and MgCO₃ in post-Jurassic deposits of the central northwestern Pacific, southern Hess Rise, DSDP Site 466.

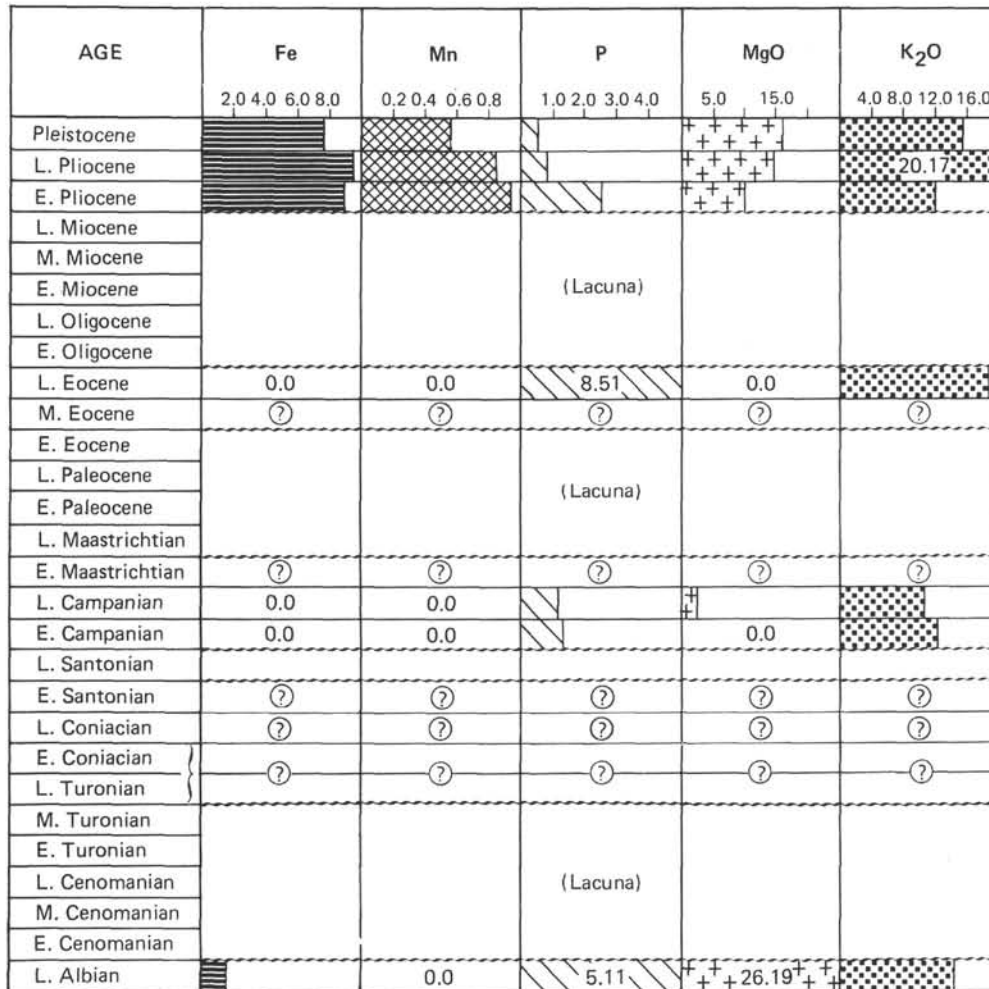


Figure 4. Distribution of average contents (wt. %, recalculated to terrigenous-free, carbonate-free, silica-free) in post-Jurassic deposits of the central northwestern Pacific, southern Hess Rise, DSDP Site 466.

and forms of their occurrence (by the results of factor analysis and mineralogy), and rates of accumulation, interpreted in the context of general information on lithology of these deposits.

The most essential geochemical features of the late Albian (early-oceanic) stage reside in the fact that the major part of the main components and heavy metals accumulated in a form of basaltic volcanics, partially altered into Fe-montmorillonite, and mixed-layer montmorillonite-illite. The volcanogenic products are closely bound to sapropelic organic matter. The geochemistry of clastic carbonate sedimentation is less pronounced. The sediments were accumulated in a relatively shallow basin with stagnant bottom waters.

An Early Cenomanian/Middle Turonian hiatus is of a regional nature within Hess Rise.

Geochemical parameters of nannofossil sediments of the Late Cretaceous (late Turonian/early Maastrichtian) are very close to those of pelagic carbonate oozes of the open ocean. Relatively high rates of sedimentation in the late Turonian-early Santonian can be explained by the assumption that during this interval southern Hess Rise occupied the equatorial zone of high

biological productivity, with northward movement of the Pacific Plate (Lancelot and Larson, 1975; Lancelot, 1978; van Andel, 1974).

During the Tertiary-Quaternary, a late Maastrichtian/early Eocene hiatus is of a regional nature, reflecting a sharp change in global oceanic circulation.

The middle-late Eocene saw accumulation of pelagic carbonate nannofossil sediments with higher concentration of products remaining after dissolution: Mn-hydroxides and Al₂O₃ and P compounds.

An early Oligocene/late Miocene hiatus is of a wide regional nature in the central northwestern Pacific.

The Early Pliocene-Pleistocene saw accumulation of nannofossil carbonate pelagic oozes, with peculiar, relatively high concentrations of SiO₂, Al₂O₃, Fe, Mn, and associated heavy metals, increasing toward the Pleistocene, because of intensification of island volcanism; sedimentation took place in the northern oligotrophic zone of the Pacific.

Thus, for the studied region of Hess Rise, as for some other regions of the northwestern Pacific, the identified geochemical stages in the history of post-Jurassic sedimentation reflect the evolution of the basin from condi-

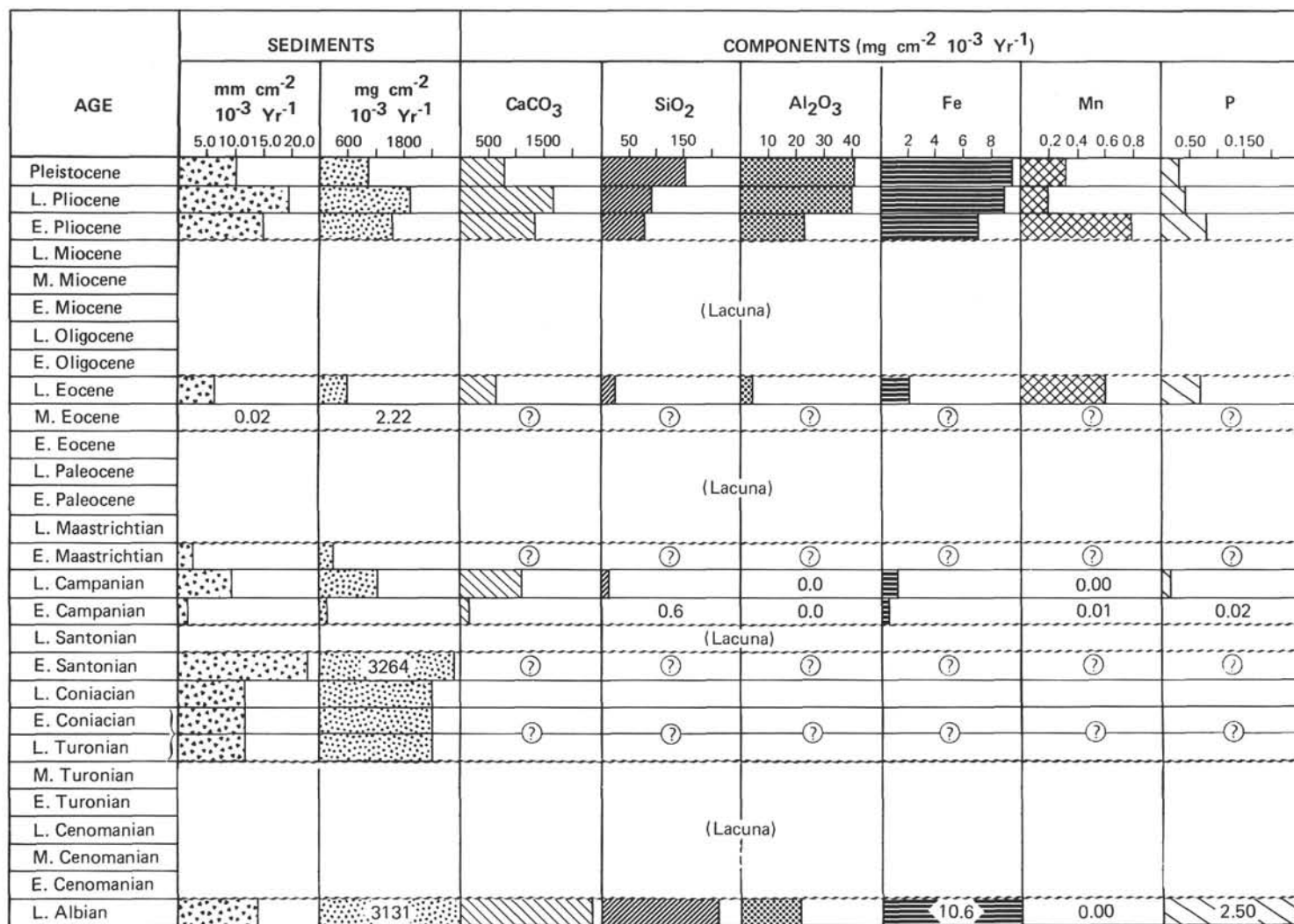


Figure 5. Distribution of average rates of sedimentation and accumulation of CaCO_3 , SiO_2 , Al_2O_3 , Fe, Mn, and P in post-Jurassic deposits of the central northwestern Pacific, southern Hess Rise, DSDP Site 466.

tions of relatively shallow-water sedimentation with stagnant bottom waters, accumulation of sapropelic sediments, and the essential influence of volcanism, to pelagic sedimentation of the open ocean.

ACKNOWLEDGMENTS

The author takes this opportunity to express his gratitude to his colleagues in the Geological Institute of the U.S.S.R. Academy of Sciences: P. K. Ryabushkin, D. A. Kazimirov, N. I. Kartoshkina, and N. Yu. Vlasova, for assistance in processing the analytical data by computer, recalculation of analyses, and making the manuscript readable; V. A. Drits, B. A. Sakhorov, and T. G. Eliseeva, for X-ray structural analysis; D. Ya Choporov, for control over analytical data; P. P. Timofeev and V. I. Koporulin, for provided materials and discussion of the results; V. S. Zelinsky, and L. M. Ruleva, for assistance in drawings; G. N. Surovtseva, and I. G. Sheremet, for translation.

Critical review of the paper and comments by N. G. Brodskaya and A. G. Kossowskaya improved the work.

REFERENCES

- Arrhenius, G., 1963. Pelagic sediments. In Hill, M. N. (Ed.), *The Sea* (Vol. 3): New York (Interscience), 655-727.
- , 1967. Deep sea sedimentation: a critical review of U.S. works. *Trans. Am. Geophys. Union*, 48:604-631.
- Bezrukov, P. L., and Romankevich, E. A., 1970. Rate of sedimentation in Pacific ocean. In Bezrukov, P. L. (Ed.), *Pacific Ocean: Sedimentation in Pacific Ocean* (Vol. 2): Moscow (Nauka), 288-300.
- Bogdanov, Yu. A., and Chekhovskikh, E. M., 1979. Rates of sedimentation and absolute masses. In Smirnov, V. I. (Ed.), *Metalliferous Sediments of South-Eastern Pacific Ocean*: Moscow (Nauka), p. 280.
- Davis, J. C., 1973. *Statistics and Data Analysis in Geology*: New York (Wiley).
- Harman, H. H., 1967. *Modern Factor Analysis*. Chicago (Univ. of Chicago Press).
- Kirkpatrick, J., 1979. Interlaboratory comparison of Leg 46 basalt standards. In Dmitriev, L., Heirtzler, J., et al., *Init. Repts. DSDP*, 46: Washington (U.S. Govt. Printing Office), 293-297.
- Lancelot, Y., 1978. Relations entre évolution sédimentaire et tectonique de la Plaque Pacifique depuis la Crétacé inférieur. "*Mém. Soc. Géol. France*," 57(134):40.
- Lancelot, Y., and Larson, R. L., 1975. Sedimentary and tectonic evolution of the northwestern Pacific. In Larson, R. L., Moberly R., et al., *Init. Repts. DSDP*, 32: Washington (U.S. Govt. Printing Office), 925-939.
- Lisitzin, A. P., 1974. *Sedimentation in Oceans*: Moscow (Nauka).
- , 1978. *Processes of Oceanic Sedimentation: Lithology and Geochemistry*. Moscow (Nauka).
- Luyendyk, B. P., Forsyth, D., and Phillips, J. O., 1972. Experimental approach to the paleocirculation of the oceanic surface water. *Geol. Soc. Am. Bull.*, 83:2649-2664.
- MacArthur, J. M., and Elderfield, H., 1977. Metal accumulation rates in sediments from Mid-Indian Oceanic Ridge and Marie Celeste Fracture Zone. *Nature*, 266:437-439.
- Tiercelin, J. J., and Faure, H., 1978. Rates of sedimentation and vertical subsidence in neorifts and paleorifts. *Tectonics and Geophysics of Continental Rifts* (Vol. 2): Moscow (Dordrecht), 41-47.
- van Andel, Tj. H., 1974. Cenozoic migration of the Pacific Plate, northward shift of the axis of deposition and paleobathymetry of the Central Equatorial Pacific. *Geology*, 2:507-510.
- Varentsov, I. M., and Blazhchishin, A. I., 1976. Ferromanganese nodules. *Geology of Baltic Sea*: Vilnius (Mokslas), pp. 307-348.
- Zolotarev, B. P., and Choporov, D. Ya., 1978. Petrochemistry of basalts D/V *Glomar Challenger*, Leg 45, Holes 395, 395A, 396. In Melson, W. G., Rabinowitz, P. D., et al., *Init. Repts. DSDP*, 45: Washington (U.S. Govt. Printing Office), 479-492.